PHYSICAL REVIEW B VOLUME 49, NUMBER 13 1 APRIL 1994-I

Rapid Communications

Rapid Communications are intended for the accelerated publication of important new results and are therefore given priority treatment both in the editorial office and in production. A Rapid Communication in **Physical Review B** *should be no longer than four printed pages and must be accompanied by an abstract. Page proofs are sent to authors.*

Pressure-induced level crossing in $KZnF_3:Cr^{3+}$

P. T. C. Freire, O. Pilla,* and V. Lemos
Instituto de Física "Gleb Wataghin," Universidade Estadual de Campinas (UNICAMP), Caixa Postal 6165, 13083-970 Campinas, São Paulo, Brazil
(Received 9 December 1993)

We report detection of the low-field–high-field transition in $KZnF_3:Cr^{3+}$, induced by external pressure, through photoluminescence measurements at both room temperature and $T = 90$ K. Direct measurement of the lowest electronic level separation Δ was accomplished through lower-temperature experiments. Pressure coefficients of Δ and values of the crystal-field and covalence quenched free-ion parameters are given.

The success of the crystal-field approximation in predicting the electronic level diagrams of ions of octahedral sites in a variety of host crystals is well known.[1] Of present interest are the lowest-lying levels of Cr^{3+} ions, which can be either $^4T_2$ or ^2E depending on the crystal-field strength. The signature of the $^4T_2$ emission energy is its high sensitivity to the crystal field while the ^2E emission energy, on the other hand, is constant. This energy sensitivity is a consequence of the symmetries: both the ^2E state and the ground state $^4A_2$ arise from the $(t_{2g})^3$ electronic configuration, while the $^4T_2$ state derives from the $(t_{2g})^2 e_g$ configuration.[2] The application of Cr^{3+}-doped crystals to wide-band, tunable, high-power lasers[3,4] motivated recent investigations.[5–10] The electronic levels acting as laser levels produce a broad absorption band, due to phonon-assisted $^4T_2 \longrightarrow {}^4A_2$ transitions. The corresponding emission, in the near-infrared spectral region, can be shifted toward the visible region by application of external pressure. The limit is established by the crossing of $^4T_2$ and ^2E levels and therefore, it is important to study the behavior of these levels with pressure. The separation of the zero-vibration states of these levels is usually labeled Δ (in the absence of lower symmetry fields and spin-orbit coupling). The few experimental results in this area are restricted to small-Δ crystals and room-temperature (RT) measurements.[2,7] Since the zero-phonon line merges into the broad $^4T_2$ emission band at RT, these studies do not directly measure Δ. It is worthwhile to note that transitions between $^4T_2$ and ^2E are nonradiative; otherwise detection would be straightforward or could be improved by new developments.[11]

Here, we report on the crossing of the electronic levels by measurements of luminescence at both low temperature and RT. An intermediate crystal-field material, $KZnF_3:Cr^{3+}$, served this purpose. This material exhibits pure $^4T_2$ behavior at low pressures (for either temperature value), but the crossing is within the working range of available cells. The room-temperature results allowed observation of the crossing through the behavior of broad emission bands. At low-temperature zero-phonon lines (ZPLs) were used. As a result, the pressure that reduces the separation Δ to zero, P_c, was determined at both temperatures. We also discuss the determination of the crystal-field parameter Dq and the covalence quenched free-ion parameters B, C, and ζ.

Single crystals of $KZnF_3:Cr^{3+}$ were grown by using Bridgman's method, from a stoichiometric proportion of KF and ZnF^{2+}, and doping with $CrCl_3$ (3%). The crystals thus prepared have perovskite structure with three different centers of Cr^{3+}. Previous electronic paramagnetic resonance (EPR) results on this material[3] indicate dominant contribution of cubic symmetry (about 90% of the centers), and a considerable amount of trigonally distorted centers ($\sim$ 10%). Tetragonal symmetry centers occur with much lower abundance. A thin, (001) oriented slice was cut, and polished to 70 μm slabs from which the samples were selected. A Membrane Diamond Anvil Cell[12] (MDAC) loaded with Ar was employed to produce hydrostatic pressure. The shift of the R line of $MgO:V^{2+}$ served the purpose of calibrating the pressure. These shifts were measured using the line 877.67 nm of a Kr lamp as reference and the rate of 5.45 Å GPa^{-1}.[2] Correction for low-temperature shifts were based on results of Ref. 13. The excitation was achieved with the 514.5 nm line of an Ar ion laser, the 632.8 nm line of a He-Ne laser or the 628.0 nm line of a cw tunable dye laser operating with DCM dye. Analysis was made with a Spex Triplemate 1877 linked to a Hamamatsu R943–02 photomultiplier and photon counting detection.

The distinction between low-field and high-field octahedral chromium complexes is the sign of the separation Δ. For weak crystal fields, the $^4T_2$ excited state lies below the ^2E state and Δ is negative. For stronger crystal fields, the minimum energy state is ^2E and Δ is positive. The characteristic of $^4T_2 \longrightarrow {}^4A_2$ transitions is the high sensitivity of the emission energy to crystal-

field variation. The $^2E \longrightarrow {}^4A_2$ transition energies, on the other hand, hardly change with crystal field. As a consequence, the shifts of the $^4T_2$ emission are responsible for the Δ dependence on crystal field within a few percent. The crystal-field parameter is a strongly varying function of pressure, but a slowly varying function of temperature, over the region currently investigated (0–300 K).[8] To analyze the effect of pressure on Δ, two values of temperature were selected, room temperature and $T = 90$ K. Figure 1 shows photoluminescence spectra of $KZnF_3:Cr^{3+}$ taken at atmospheric pressure (lower curve) and at $P = 12.5$ GPa (higher curve), both at room temperature. Since the magnitude of Δ at ambient conditions is much larger than the spin-orbit interaction energy, the emission labelled 0.0 GPa in Fig. 1 can be assumed to be due to pure spin allowed $^4T_2 \longrightarrow {}^4A_2$ transitions. On increasing pressure, the broadband was observed to shift to higher energies at a constant rate up to pressures of about 8 GPa. The line shape of this band is the well-known Pekarian curve and remains unaltered on compression, although its integrated intensity decreases considerably. On increasing further the pressure, the emission spectrum changes qualitatively. Above 9 GPa it consists of a highly structured region superimposed on a broadband emission of symmetrical line shape. Figure 1, upper curve, illustrates such a spectrum, for the pressure value of 12.5 GPa. Three narrow lines are dominant in the sharp emission region peaked at (15 090 ± 2) cm^{-1}, (14 850 ± 5) cm^{-1}, and (14 735 ± 2) cm^{-1}. These lines are attributed to the zero-phonon R line due to $^2E \longrightarrow {}^4A_2$ transition (the highest energy line) followed by its phonon sidebands (lower energies). Even if Cr^{3+} centers in cubic, trigonal and tetragonal sites contribute to the total emission of Fig. 1, in the spectrum at 12.5 GPa the R line does not resolve into fine structures, its width at half maximum being about 30 cm^{-1}. In addition to the sharp peaks a broadband contribution is observed peaking about 1100 cm^{-1} from the R line. At this temperature we are not able to measure directly Δ since the $^4T_2$-ZPL is not observed being merged into the broadband. Nevertheless, we can estimate Δ assuming for the $^4T_2$-ZPL a displacement with pressure equal to the one measured for the emission maximum. This assumption turns out to be strictly true at $T = 90$ K, as can be checked through the following discussion. The ^2E-ZPL shift on pressure, on the other hand, is negligible in the scale of interest. Therefore, this shift should be represented as a straight line parallel to the abscissa in an energy vs pressure plot. Considering the ZPL positions relative to the broadband maxima as the same regardless of the pressure value, the broadband positions can be used to define the crossing (in the lack of absolute values for ZPLs). Pursuing this idea, the broadband maxima, were plotted vs pressure in the inset of Fig. 1 (full circles). The open symbols represent sharp line positions plotted here to show the behavior of R line emission. The solid line is a least-squares fitting of the data in range (0–8) GPa to the function:

$$E(^4T_2 \longrightarrow {}^4A_2) = E_0 + \alpha P. \quad (1)$$

The fitting numerical results are listed in Table I. The dotted line in the inset of Fig. 1 was drawn through the experimental points as a guide to the eyes. These lines cross at (8.0 ± 0.2) GPa, which we take as the crossing pressure P_c. The uncertainty in the value of P_c was taken as the total increase in linewidth of the $MgO:V^{2+}$ R line, assumed to be due to nonhydrostaticity only. At the value P_c, $\Delta = 0$ and this, in turn, gives the dependence of Δ with pressure as

$$\Delta = \Delta_0 + \alpha P, \quad (2)$$

where the value $\Delta_0 = -(14.3 \pm 0.9) \times 10^2$ cm^{-1} gives the estimated separation between ^2E and $^4T_2$ levels at ambient pressure and room temperature.

Low-temperature and simultaneous compression were observed to reduce the integrated intensity of the broadband emission drastically. At $T = 90$ K, for instance, there was hardly any broadband emission for pressure values in the high-field region. To find the level crossing in this case, we analyzed the sharp line spectra. Observation of line spectra was accomplished using as excitation a red line nearly coinciding with the maxima in the absorption spectrum of the Cr^{3+} levels. Lumines-

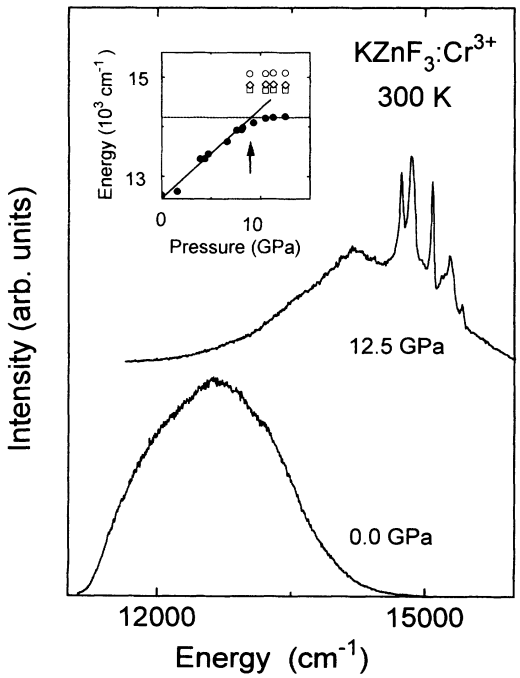

FIG. 1. Photoluminescence spectra in low-field and high-field regimes, taken with $\lambda_{ex} = 514.5$ nm. The inset illustrate the transition between these regimes.

TABLE I. Pressure coefficients from least-squares fittings of experimental data on $^4T_2 \longrightarrow {}^4A_2$ emission to Eq. (1). The error of α is the standard deviation of the fitting.

Feature	T (K)	E_0 (cm^{-1})	α (cm^{-1} GPa^{-1})
Broadband	300	12 560 ± 60	179 ± 7
Broadband	90	12 869 ± 60	167 ± 2
C line	90	14 089 ± 1	167 ± 9

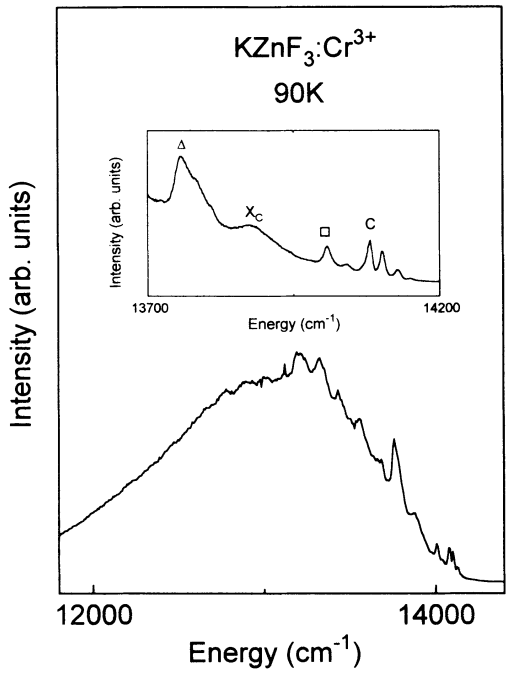

FIG. 2. Photoluminescence spectrum (λ_{ex} = 628.0 nm) at atmospheric pressure. The inset shows the assignments of the sharp line spectrum.

cence measurements performed at atmospheric pressure and T = 90 K with λ_{ex} = 628.0 nm resulted in the spectrum displayed in Fig. 2. Sharp lines are clearly seen on the higher-energy side of the broadband emission. To identify the several lines, we compare their energy with previous published data.[5,6] The inset in Fig. 2, shows the labeling adopted here for the most prominent structures. According to Ref. 6 the symbols △ and □, are for the lower symmetry crystal fields of trigonal and tetragonal centers, respectively. C stands for cubic ZPL and X_c for its one-phonon sideband. The energy positions of these lines are listed in Table II. Also listed are their values according to Refs. 5 and 6. The first reports the spin-orbit splittings of the cubic $^4T_2$-ZPL by using the irreducible representations of the group O_h, to denote the components of the quartet. These notations are in parentheses in the first column of Table II.

Figure 3 illustrates the evolution of luminescence spectra with pressure at low temperature for which λ_{ex} = 632.8 nm was used. The spectrum taken at atmospheric pressure, labeled 0.0 GPa in this figure, allows for the observation of both trigonal and cubic ZPLs, besides the broadband, from $^4T_2$ emission. As pressure increases there is a marked decrease in the integrated intensity of the whole structure, but the narrow C lines are always present in the spectra. Both features, broadband and C line shift linearly with pressure, at the same rate within experimental errors, up to ~ 5 GPa. Also noticeable is the fact that the spectra remain qualitatively the same in the pressure range (0–5) GPa. A qualitative change happens to occur at a higher pressure value with the broadband disappearing, and a sharp line spectrum arising. This behavior is shown in Fig. 3, where the spectra taken at atmospheric pressure and P = 10.0

TABLE II. Line spectra assignments corresponding to $^4T_2 \longrightarrow {}^4A_2$ electronic transitions of Cr^{3+} level, at atmospheric pressure.

Type	E (cm^{-1})[a] T = 90 K	E (cm^{-1})[b] T = 4.2 K	E (cm^{-1})[c] T = 10 K
△	13765 ± 2	13766	13765
X_c	13880 ± 4	13878	13891
□	14016 ± 1 14052 ± 1	14016	14016
$C(\Gamma_7)$	14089 ± 1	14089	14091
(Γ_8)	14110 ± 1	14110	
(Γ_8')	14136 ± 1	14138	
(Γ_6)		14159	

[a]Present results.
[b]Reference 5.
[c]Reference 6.

GPa are compared. The highest energy peak, labeled C in the upper curve of Fig. 3 is assumed to correspond to $^2E \longrightarrow {}^4A_2$ cubic symmetry ZPL. This is consistent with the fact that higher symmetry centers emit at higher energies. The several narrow lines at lower energies have contributions from other symmetry centers. The detailed assignments of these lines are going to be reported elsewhere. The peak positions are plotted vs pressure in the inset of Fig. 3. In this plot, the symbol and line notation is the same as that for the RT results. The open circles at the lower pressure region are the emission energies of cubic $^4T_2$-ZPL. At 90 K, it is well located, allowing for the direct determination of the pressure of crossing P_c.

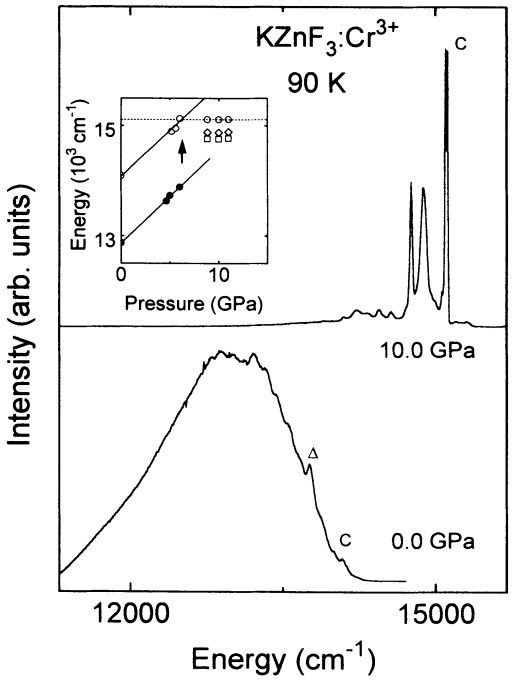

FIG. 3. Low-temperature evolution of luminescence spectra with pressure. The inset shows the energy dependence on pressure. The arrow indicates the crossing of electronic levels.

This value, indicated in the inset of Fig. 3 by an arrow, is $P_c = (6.2 \pm 0.2)$ GPa. The pressure coefficients resulting from the fittings (solid lines in the inset), are given in Table I. The same linear coefficient was obtained for both features, broadband and C line, at $T = 90$ K. From the plot we also extracted the value $\Delta_0 = -(10.3 \pm 0.9) \times 10^2$ cm^{-1}, which together with Eq. (2) and α value of Table I describe the behavior of $^2E \longrightarrow {}^4A_2$ separation energy at $T = 90$ K.

Comparing results of low temperature and RT improves understanding of the subject. The mechanism of decreasing emission intensity on compression, for instance, can be explained in terms of spin-orbit coupling effects. The zero-phonon $^2E \longrightarrow {}^4A_2$ transition, is magnetic dipole allowed and electric dipole forbidden in the cubic symmetry representation. Intensity of the transition is gained through admixture of states $^4T_2$ and ^2E by spin-orbit interaction. The $^2E \longrightarrow {}^4A_2$ transition probability is then given by[14]

$$\frac{1}{\tau} = d^2 \frac{1}{\tau(^4T_2)} \tag{3}$$

with

$$d = \sqrt{\frac{1}{2}}(1 - \Delta/\sqrt{4|V_{SO}|^2 + \Delta^2})^{1/2}. \tag{4}$$

These kind of relations can be used to estimate the dependence of total decay rate as a fraction of a pure $^4T_2 \longrightarrow {}^4A_2$ transition rate $(1/\tau_0)$ on temperature. This was done before in the case of a small positive Δ crystal by Healy *et al.*,[9] and their results are going to be used here in our qualitative analysis. The decay time calculated at low temperature increases by an amount of ~100% on changing from $\Delta \sim -1000$ to $\Delta = 0$ (see Fig. 4 of Ref. 9). Conversely, the radiative decay rate can be assumed to decrease by the same amount. At room temperature, on the other hand, the increase in time decay is $\sim 0.33\tau_0$, which, in turn, leads to a decrease of only ~33% on the decay rate on going from $\Delta = -1000$ cm^{-1} to $\Delta = 0$. Therefore, the radiative decay decrease at low temperature is about three times larger than at RT. This comparison explains why the transition from low field to high field is much better defined at low temperature.

Crystal-field theory parameters can be improved when evaluated from pressure experiments. The crystal-field strength Dq and one of Racah's coefficients, B, are obtained straightforwardly from absorption spectra.[15] The difficulty arises in determining the parameter C for low crystal-field materials. Usually this value is roughly estimated in intermediate field systems by the position of ^2E Fano resonances.[16] Pressure, disclosing the ^2E emission, yield a direct observation of its energy. Since ^2E emission is a sharp line the accuracy in its position is larger, and also in B, C and ζ, in accordance. Our result for the $^2E \longrightarrow {}^4A_2$ energy (15 113 $\pm$ 2) cm^{-1} yields $B = (713 \pm 1)$ cm^{-1}, $C = (3211 \pm 5)$ cm^{-1}, and $\zeta = (213.7 \pm 0.4)$ cm^{-1}. These values are reduced compared to previous published data,[5] on the same system.

High pressure luminescence measurements performed at RT and 90 K, yield the determination of the crossing of the lowest lying levels of Cr^{3+} in the host crystal $KZnF_3$. The crossing pressure at room temperature $P_c = (8.0 \pm 0.2)$ GPa was determined on the basis of the behavior of the broadband $^4T_2$ emission. The 90 K data, on the other hand, allowed observation of the cubic ZPL in the whole pressure range. Hence, these results give the direct measurement of the separation between ^2E and $^4T_2$ zero-vibration states. The value of the crossing pressure at this temperature was found to be (6.2 $\pm$ 0.2) GPa. To our knowledge, no experimental data accomplished a direct observation of Δ before. Our results also yielded the value of Racah's parameters from crystal-field theory, with improved accuracy. These results are important to the knowledge of lasing properties of solid state laser materials.

We are greatly indebted to Professor U. Dürr for providing the samples used in these experiments and to Professor M. Montagna for useful discussions. We are grateful for financial support from Conselho Nacional de Desenvolvimento Científico e Tecnológico (CNPq), Fundação de Amparo à Pesquisa do Estado de São Paulo (FAPESP), Fundo de Apoio ao Ensino e à Pesquisa (FAEP/ UNICAMP), and Consiglio Nazionale delle Ricerche (CNR).

* On leave from Università degli Studi di Trento, Trento, Italy.

[1] Y. Tanabe and S. Sugano, J. Phys. Soc. Jpn. **9**, 766 (1954).
[2] D. de Viry, J.P. Denis, N. Tercier, and B. Blanzat, Solid State Commun. **63**, 1183 (1987).
[3] U. Brauch and U. Dürr, Optics Commun. **49**, 61 (1984).
[4] J. Buchert and R.R. Alfano, Laser Focus/Electro-Optics **19**, 117 (1983).
[5] O. Pilla, E. Galvanetto, M. Montagna, and G. Viliani, Phys. Rev. B **38**, 3477 (1988); E. Galvanetto, thesis, Università di Trento, 1988.
[6] Y. Vaills, J.Y. Buzaré, and M. Rousseau, J. Phys.: Condens. Matter **2**, 3997 (1990).
[7] J.F. Dolan, L.A. Kappers, and R.H. Bartram, Phys. Rev. B **33**, 7339 (1986).
[8] C.J. Donnelly, S.M. Healy, T.J. Glynn, G.F. Imbusch, and G.P. Morgan, J. Lumin. **42**, 119 (1988).
[9] S.M. Healy, C.J. Donnelly, T.J. Glynn, G.F. Imbusch, and G.P. Morgan, J. Lumin. **46**, 1 (1990).
[10] C.J. Donnelly, T.J. Glynn, G.P. Morgan, and G.F. Imbusch, J. Lumin. **48 & 49**, 283 (1991).
[11] D.Y. Jeon, H.P. Gislason, and G.D. Watkins, Phys. Rev. B **48**,7872 (1993).
[12] R. Letoullec, J.P. Pinceaux, and P. Loubeyre, *High Pressure Science and Technology*, edited by M. Ross (Gordon and Breach, London, 1990), Vol. 5, p. 871.
[13] B. di Bartolo and R. Peccei, Phys. Rev. **137**, A1770 (1965).
[14] B. Struve and G. Huber, Appl. Phys. B **36**, 195 (1985).
[15] J.C. Eisenstein, J. Chem. Phys. **34**, 1628 (1961).
[16] M.D. Sturge, H.J. Guggenheim, and M.H.L. Pryce, Phys. Rev. B **2**, 2459 (1970).